Geomorphology 273 (2016) 52–62

Contents lists available at ScienceDirect

Geomorphology

journal homepage: www.elsevier.com/locate/geomorph

The influence of human activities on morphodynamics and alteration of sediment source and sink in the Changjiang Estuary

Lei Zhu [a], Qing He [a,*], Jian Shen [b], Ya Wang [a,b]

[a] State Key Laboratory of Estuarine and Coastal Research, East China Normal University, Shanghai 200062, China
[b] Virginia Institute of Marine Science, College of William & Mary, Gloucester Point, VA 23062, United States

ARTICLE INFO

Article history:
Received 19 December 2015
Received in revised form 11 July 2016
Accepted 14 July 2016
Available online 5 August 2016

Keywords:
Morphodynamics
Erosion rate
Residual flow
Sediment source

ABSTRACT

Several works have discussed the morphological evolution in the Changjiang Estuary (CJE) in recent years. The erosion of its subaqueous delta in recent decades has been ascribed to a decline in fluvial sediment input. However, the interaction between the reduction of riverine sediment load and human activities in the estuary that could have caused morphological change has not been considered. In this work we provide evidence on the morphological evolution around the delta front zone since 1986 and use a numerical model to explore the correlation between the change in hydrodynamics and the evolution pattern. Bathymetric data analysis suggests a decrease of net accretion rate from 16.7 mm/year (1986–1997) to 9.1 mm/year (1997–2010) in the study area. Spatially, the tidal flats accreted whereas the subaqueous delta switched from deposition between 1986 and 1997 to erosion between 1997 and 2010. We used two indicators, tidal energy dissipation and erosion rate, to quantify the change in hydrodynamics and found that the erosion of the subaqueous delta in recent decades can readily be explained by the alteration of the hydrodynamics. The newly built navigation training works in the North Passage had a significant effect on the estuarine hydrodynamics, resulting in a local morphological adjustment. This erosion generated a new source of sediments to maintain the high suspended sediment concentration and tidal flat progradation. The erosion of the subaqueous delta may continue and gradually slow down until the altered hydrodynamics and morphology reach an equilibrium state in the future.

© 2016 Elsevier B.V. All rights reserved.

1. Introduction

An estuary is a transition zone between riverine and marine environments. Thus, estuary morphological change is sensitive to both human activities in the drainage area and adjacent coasts. Hydrological dams, soil and water conservation, and sand mining have resulted in a decrease in fluvial sediment load. The sediment delivery to deltas worldwide has been reduced during the past 50 years due to upstream damming (Syvitski et al., 2009). For example, a 50% reduction in suspended sediment load in the Mississippi River during the last few decades has been observed, which resulted in unsuitable conditions for wetland vegetation, yielding the loss of marsh habitat (Kennish, 2001). Human activities in estuaries, such as training wall construction, channel dredging, and land reclamation, can cause dramatic changes in the hydrodynamics, sediment transport, and morphological evolution patterns of estuaries (Sherwood et al., 1990; Nichols and Howard-Strobel, 1991; Spearman et al., 1998; Blott et al., 2006; Talke et al., 2009).

The Changjiang River has become a focal point for research because of the construction of the Three Gorges Dam (TGD). The effect of the TGD on river ecology and the geological disaster in the reservoir area after impoundment are the main concerns (Stone, 2008). Apart from this, the response of the Changjiang subaqueous delta to the impoundment of sediment by the TGD is also a topic of interest. Yang et al. (2003) predicted the potential morphological evolution after the TGD and concluded that the Changjiang Estuary (CJE) will become eroded once the annual sediment load is $<260 \times 10^6$ t/year. Similar critical values of 395×10^6 t/year and 184×10^6 t/year were reported based on linear regression analysis between river-born sediment and erosion/accretion volume of the delta (Chen and Zong, 1998; Li et al., 2004). However, these studies only covered part of the delta (<2000 km^2), and may not be representative of the entire delta. The sediment load from the river to the CJE has decreased since the 1980s and a notable decrease occurred after the impoundment of the TGD in 2003 (Gao et al., 2011). Even with a sharp decrease in sediment load, a recent study showed that erosion only occurred locally and there is no obvious trend of erosion within the CJE (Dai et al., 2014). Thus it is still debatable to what degree the morphology has responded to reduced riverine sediment load, and there is no consensus on any persistent evolution pattern. The underlying mechanisms of estuarine morphological changes are also not fully understood.

* Corresponding author.
E-mail address: qinghe@sklec.ecnu.edu.cn (Q. He).

http://dx.doi.org/10.1016/j.geomorph.2016.07.025
0169-555X/© 2016 Elsevier B.V. All rights reserved.

The CJE is a large estuary with complex dynamics, thus it is difficult to distinguish the impacts of the changes in the upstream river basin from changes within the estuary (Chen et al., 1999). Huo et al. (2010) examined the long-term morphological evolution of Nanhui Shoal (Fig. 1) and found that the evolution of Nanhui Shoal is highly sensitive to the flow and sediment diversion in the upstream channels. Furthermore, the hydrodynamics of the CJE are complex as they are strongly influenced by the huge river flow as well as strong tidal currents and waves, which result in spatial and temporal variations of suspended sediment concentration (Shen et al., 2013).

In addition to the decrease in sediment supply to the estuary, the estuary has been influenced by the building of large infrastructures. Such changes can alter the dynamics of the estuary, resulting in a change of sediment transport processes (Xu et al., 2009; Wu et al., 2012; Ma et al., 2013). The recently observed transformation of a region of historical deposition to net erosion following construction of the TGD suggests a change from a sediment sink to a sediment source in the CJE (Liu et al., 2012). However, the cause of this change is not fully understood.

So far many studies of estuary dynamics and sediment transport processes in the CJE have been conducted, most of which focus on sediment dynamics and transport in the channels of the estuary. The effect of interactions between natural evolutionary processes and human impact on the recent change of the delta has not been studied in full. We hypothesize that local human intervention in the CJE in recent years has altered hydrodynamics to a major degree, which have contributed to the recent change of the morphological evolution pattern of the estuary. The questions as to how hydrodynamic conditions have been changed in response to evolved morphology and engineering works and how a change in hydrodynamic conditions contributes to the shifting of the sediment sources and sinks are insufficiently studied. Thereby, the objectives of this study are to investigate: 1) the correlation between the change in hydrodynamics and the change of erosion and deposition patterns; 2) the contribution of the change in dynamic conditions to the alteration of sediment transport processes in the estuary; and 3) the causes of possible switching between sediment sources and sinks under the influence of bathymetric change and man-made construction. We used a numerical model to reproduce the hydrodynamics under varying bathymetries. Two indicators, tidal energy dissipation and erosion rate, were applied to quantify the change in hydrodynamics and we detected the interaction between hydrodynamics and morphological evolution. In that sense, this work enables us to establish the main factors that control morphological evolution and the change of the large-scale net sediment transport pattern on a decadal time scale.

2. Study site

The Changjiang River is the largest river leading to the Western Pacific. The annual river discharge and suspended sediment load in the period 1950–2010 are approximately 900×10^9 m^3/year and 390×10^6 t/year at Datong Gauge Station, about 640 km upstream of the river mouth, where daily discharge is measured. About half of the total sediment load is deposited within the estuary (Milliman et al., 1985; Liu et al., 2006). The comparison of the present coastline with the ancient coastline suggests that about 12,000 km^2 of estuarine waters have become land in the past 2000–3000 years due to deposition of riverine sediment (Chen et al., 1988; Yang et al., 2001).

The CJE is first divided into the South Branch and the North Branch by Chongming Island, and then the South Branch is divided into the South Channel and the North Channel by Changxing and Hengsha Islands. Finally the South Channel branches into the South Passage and the North Passage by Jiuduansha Shoal (Fig. 1). The turbidity maximum zone, formed under the combined effects of gravitational circulation (Shen et al., 1986a, b), sediment flocculation (Tang et al., 2008) and sediment resuspension (Li and Zhang, 1998), is located in the lower reach of North Channel, North Passage and South Passage. The CJE is a mesotidal regime. The mean tidal range at Zhongjun tide-gauge station is 2.66 m and the tidal range decreases further upstream along the South Branch.

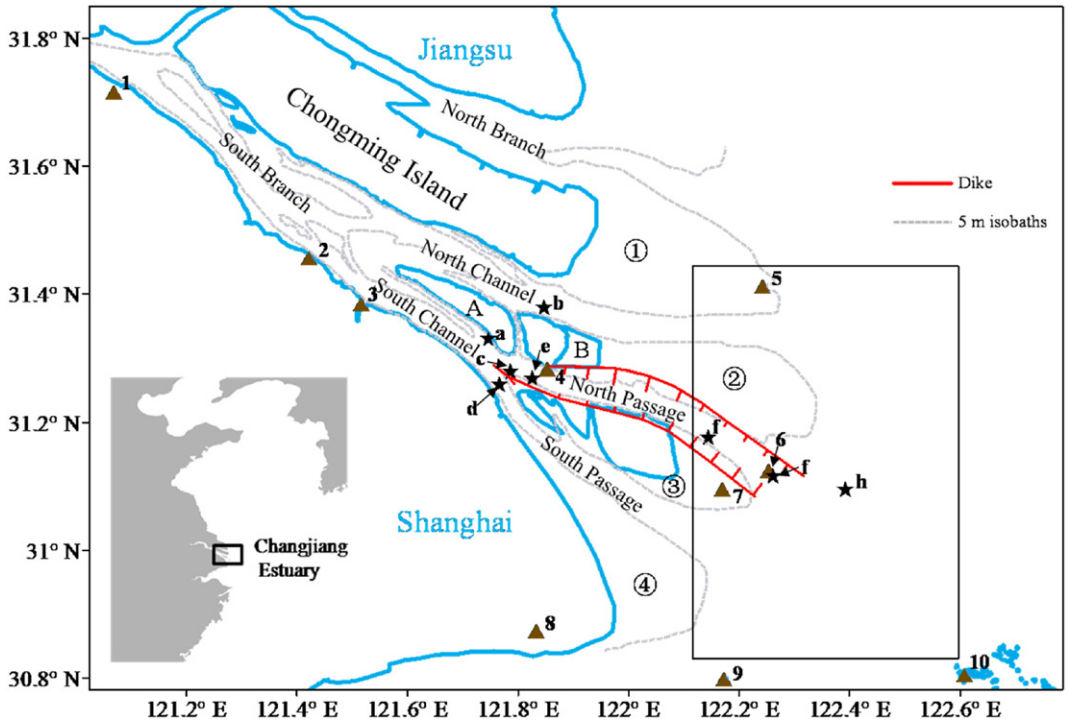

Fig. 1. Study area and measurement sites (A. Changxing Island, B. Hengsha Island; 1. Baimao, 2. Shidongkou, 3. Wusong, 4. Hengsha, 5. Sheshan, 6. Niupijiao, 7. Jiuduandong, 8. Luchaogang, 9. Dajishan; a. NG2, b. BG1, c. CB1, d. NC1, e. CS0, f. CS3, g. CS4, h. CS5; the rectangle is where the morphological evolution is detected; ①: Chongming East Shoal, ②: Hengsha East Shoal, ③: Jiuduansha Shoal, ④: Nanhui Shoal).

The subaqueous delta of the CJE extends seaward with a water depth ranging from 5–10 m to about 30–50 m outside the river mouth (Chen, 2007). >50,000 dams and reservoirs have been constructed during the past 50 years. Reduction in sediment supply is a great concern on the delta stability. Especially after the TGD project in 2003, a further decline in the sediment load has been observed (Fig. 2) at Datong Gauge Station. Coarser sediment was impounded behind the dams, the median grain size of sediment transported downstream has decreased from 17 μm before 2003 to 10 μm after the construction of the TGD (Tang, 2007). A large scale Deep Waterway Project (DWP) was constructed to improve the navigable capacity during 1998–2010. It consists of two along-channel training walls, nineteen groins and diversion works at the inlet. The navigation channel is about 50 km long, 350–400 m wide, and 12.5 m deep (Fig. 1). The engineering construction directly influences the circulation and dynamics in the North Passage and even the estuary system. Several studies were conducted to investigate changes of hydrodynamic conditions and the sediment transport pattern. For example, the flow pattern along the North Passage changed from a rotational flow into a bi-directional flow (Hu and Ding, 2009) and large eddies have been generated inside the embayments formed by the dike-groin structures (Ma et al., 2011; Ge et al., 2012). Because of the increase of friction downstream of the South Channel, there is more freshwater transport through the North Channel, leading to an increase of barotropic pressure in the North Channel (Wang et al., 2010). It is expected that the significant change in hydrodynamics will alter the sediment transport and morphology.

3. Data and methods

3.1. Data source and analysis

In order to quantify the bathymetric change in the CJE delta front, we collected bathymetric data for the years of 1986, 1997 and 2010. These data were obtained from a single survey in each year and referenced to the same datum (the lowest astronomical tidal level), thus preserving consistency. The kriging method was selected as the interpolation technique since it provides a good interpolator for sparse data (Webster and Oliver, 2007). The bathymetric data were interpolated to a grid of 50 × 50 m cells to produce a DEM (Digital Elevation Model) by GIS software. Based on the data, we examined the spatial distribution pattern of erosion and deposition between 1986 and 2010, and estimated the sediment volume changes.

To investigate the temporal trends of morphological evolution in the subaqueous delta of CJE, we compared the bathymetries of 1986, 1997 and 2010 within a 3140 km^2 region. The study area is bounded by 30° 50.52′ N to 31°28′ N and 122°7′ E to 122°36′ E (Fig. 1). The western boundary is the four main shoals of the CJE and the eastern boundary extends to the 20-m isobaths of the delta. >95% of the water from the river discharges to the East China Sea through this area (Chen et al., 1988).

3.2. Model set-up

The Environmental Fluid Dynamics Code (EFDC) model, developed by Hamrick (1996), was used in this study. This model has been successfully applied to many water bodies such as estuaries, lakes, and coastal bays (Ji et al., 2001; Lin and Kuo, 2003; Park et al., 2005; Jeong et al., 2010; Xie et al., 2010) and it solves the Navier–Stokes equations with a free surface assumption. The modified Mellor and Yamada level 2.5 turbulence closure scheme was implemented in the model to obtain the vertical eddy viscosity and diffusivity (Mellor and Yamada, 1982; Galperin et al., 1988). The model domain is an extension of a previous small domain model (Wang et al., 2010, 2015) and covers the entire Bohai Sea, the Yellow Sea, and the East China Sea. A large domain model was used to remove any errors induced by the influence of the open boundary. The river boundary is located at 640 km upstream, at Datong Gauging Station, the tidal limit of the estuary. There are 25,922 cells in the horizontal plane with cell lengths varying from about 150 m to 30,000 m. Sixteen layers of water column of the same thickness using sigma coordinate were specified vertically. Open sea boundaries are forced by 9 harmonic constituents, namely M_2, S_2, N_2, K_2, O_1, K_1, P_1, M_4 and MS_4. This study focuses on the near coastal region where salinity dominates stratification and the influence of temperature on stratification is minimal. Therefore, the water temperature was treated as a constant during the model simulation for different seasons. The hydrodynamic roughness z_0, varying from 0.002 m to 0.008 m, was used in the model based on the model calibration. A time step of 30 s was used.

In the CJE, both tidal currents and wind-driven waves are responsible for generating the sediment suspension process. Previous studies show that waves are relatively weak during normal weather condition, however, they can be enhanced during typhoon and storm surges (Huang et al., 2007; Xiao et al., 2008; Kong et al., 2010). The estuary is classified as tide-dominated and mixed energy according to the shoreline classification system (Davis and Hayes, 1984; Hori et al., 2001). Compared with wave action, the interaction between river discharge and tidal currents dominates the medium- and long-term morphological evolution in the CJE (Hu et al., 2009; Liu et al., 2010a, b), on which we will focus in this study.

The model simulations were conducted for scenarios based on the bathymetries of 1986, 1997 and 2010, which represent historical bathymetry, bathymetries prior to training wall construction, and after construction of training walls, respectively. To investigate the effects of training walls, an extra scenario based on the 1997 bathymetry was conducted, in which the flow in a specified direction was blocked to represent training walls and groins. Based on the modeled hydrodynamics, we calculate tidal energy dissipation, erosion rate and residual current to investigate the change of hydrodynamics over time. In this study, we used the averaged daily discharge from 1986 to 2010 at Datong Station, which represents the mean condition of seasonal river discharge variation, to drive the model dynamics with respect to different bathymetries, which represents the mean condition of seasonal river

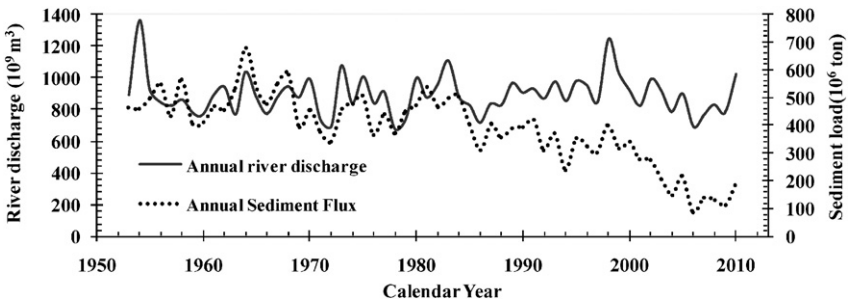

Fig. 2. Annual river discharge and sediment flux at Datong Station, 1953–2010.

discharge variation. This approach enabled us to distinguish the dynamic changes caused only by the variations in bathymetry.

Tidal energy loss can be used to measure energy available for mixing of coastal waters and to transport sediment. The work done by the bottom shear stress is mainly balanced by the energy dissipation occurring on the bottom layer, and it is proportional to the cubed velocity (Argote et al., 1995; Jayne and Laurent, 2001):

$$W = \rho_0 C_d |u_b| u_b^2 \tag{1}$$

where W is the tidal energy dissipation due to frictional drag, ρ_0 is the water density, u_b represents the velocity at the bottom layer of the model, and the drag coefficient C_d is computed as:

$$C_d = \frac{\kappa^2}{\left[\ln\left(\frac{\Delta z}{2z_0}\right)^2\right]} \tag{2}$$

where κ denotes the Von Karman constant, z_0 is the hydrodynamic roughness that has been determined in the model calibration, and Δz is the thickness of the bottom layer. In this study, we averaged the tidal dissipation over 29 days to remove the dominant tidal signals (Boon, 2004).

In order to investigate the erosion at the seabed, the well-known Partheniades (1962) formulation is applied to compute the erosion rate:

$$E = \begin{cases} M(\tau_b/\tau_e - 1) & \text{for } \tau_b > \tau_e \\ 0 & \tau_b < \tau_e \end{cases} \tag{3}$$

where $E$is the erosion rate, Mdenotes the empirical erosion parameter, $\tau_e$is the critical shear stress for erosion, bed shear stress τ_b is computed as:

$$\tau_b = \rho_0 C_d u_b^2 \tag{4}$$

In the CJE, the typical critical bottom shear stress for incipient motion of sediment is 0.5 Pa (Huang, 2003). The empirical erosion parameter is set as 5×10^{-5} kg·m^{-2}·s^{-1} since the seabed is mainly composed by mud (Mulder and Udink, 1990). The averaged erosion rate is:

$$\overline{E} = \frac{1}{nT}\int_0^{nT} E dt \tag{5}$$

where $\overline{E}$ is the averaged erosion rate, T is the period of M_2 tidal constituent, and t is the time. We averaged the erosion rate over 56 M_2 periods, approximately 29 days, to obtain the averaged erosion rate.

The residual current represents the net effects of tide-induced and baroclinically induced estuarine circulation, which is highly correlated to net sediment transport (Codiga and Aurin, 2007; Liu et al., 2011). The most common method used to calculate residual current is to average the tidal current in several tidal cycles or to use a low-pass filter to remove the periodical components. However, these approaches may not remove all the tidal signals since the period for each tidal constituent is different. In this study, we conducted other model set-ups forced only by the M_2 tidal constituent, the dominant constituent in the CJE. By doing this, we can obtain the residual current induced by the M_2 tidal constituent. Therefore, the computed residual current can represent the residual advection since the M_2 constituent is responsible for most tidal energy in the CJE and its adjacent coasts (Wu et al., 2010).

3.3. Model validation

The model was verified by its capability for tidal simulation near the coast. To examine the accuracy of the simulation, four main tidal constituents were compared with the data from the tide gauges within the CJE and Hangzhou Bay (Table 1). For the dominant M_2 constituent, the mean error for amplitude was <5% and the mean phase difference was <10°. The comparison for tidal constituents S_2, K_1, and O_1 were also performed and the results proved satisfactory.

Table 1
Calibration of the model in terms of tidal amplitudes and phases of four major tidal constituents. OBS and CAL indicate observation and calculation, respectively.

Tidal gauge	M_2 constituents						S_2 constituents					
	Amplitude			Phase			Amplitude			Phase		
	OBS (m)	CAL (m)	Error (%)	OBS (o)	CAL (o)	Error (o)	OBS (m)	CAL (m)	Error (%)	OBS (o)	CAL (o)	Error (o)
Baimao	0.86	0.84	−2%	247	246	1	0.46	0.41	−11%	120	117	3
Dajishan	1.28	1.28	0%	129	142	−13	0.62	0.65	5%	1	3	−2
Hengsha	1.06	1.14	8%	167	177	−10	0.54	0.62	15%	39	47	−8
Jiuduandong	1.23	1.24	1%	131	146	−15	0.62	0.64	3%	4	6	−2
Luchaogang	149	1.38	−7%	150	158	−8	0.67	0.72	7%	26	26	0
Lvhua	1.14	1.21	6%	107	132	−25	0.57	0.6	5%	337	348	−11
Niupijiao	1.23	1.18	−4%	127	142	−15	0.67	0.7	4%	359	360	−1
Sheshan	1.09	1.09	0%	134	145	−11	0.59	0.52	−12%	4	355	9
Shidongkou	0.90	0.95	6%	209	209	0	0.48	0.49	2%	81	79	2
Tanxushan	1.50	1.41	−6%	170	178	−8	0.65	0.77	18%	52	53	−1
Wusong	0.96	1.04	8%	195	201	−6	0.5	0.54	8%	68	72	−4

Tidal gauge	K_1 constituents						O_1 constituents					
	Amplitude			Phase			Amplitude			Phase		
	OBS (m)	CAL (m)	Error (%)	OBS (o)	CAL (o)	Error (o)	OBS (m)	CAL (m)	Error (%)	OBS (o)	CAL (o)	Error (o)
Baimao	0.27	0.27	0%	233	224	9	0.04	0.06	50%	227	224	3
Dajishan	0.35	0.36	3%	187	190	−3	0.05	0.07	40%	194	185	9
Hengsha	0.29	0.32	10%	196	205	−9	0.04	0.07	75%	209	198	11
Jiuduandong	0.30	0.34	13%	180	189	−9	0.04	0.07	75%	177	183	−6
Luchaogang	0.38	0.37	−3%	196	200	−4	0.05	0.08	60%	201	197	4
Lvhua	0.31	0.35	13%	185	183	2	0.05	0.06	20%	193	178	15
Niupijiao	0.33	0.33	0%	175	180	−5	0.04	0.06	50%	183	176	7
Sheshan	0.29	0.29	0%	170	172	−2	0.04	0.05	25%	179	175	7
Shidongkou	0.27	0.30	11%	215	212	3	0.04	0.08	100%	224	209	18
Tanxushan	0.39	0.38	−3%	207	212	−5	0.06	0.08	33%	210	210	3
Wusong	0.28	0.30	7%	210	213	−3	0.04	0.08	100%	219	214	8

In situ measurements during the summer of 2009 were available for model calibration for current and salinity. Both current and salinity measurements were conducted at 8 fixed stations, which lasted >25 h. Model results were compared with the observed data and the model skill was evaluated *via* the correlation coefficient (CC) (Oke et al., 2002; Liu et al., 2009)

$$CC = \frac{1}{N}\sum_{i=1}^{N}\frac{(m-\overline{m})(o-\overline{o})}{S_m S_o} \tag{6}$$

and skill scores (SS) (Murphy, 1988; Allen et al., 2007):

$$SS = 1-\frac{\sum_{i=1}^{N}(m-o)^2}{\sum_{i=1}^{N}(o-\overline{o})^2} \tag{7}$$

where m and o are the modeled and observed time series values, which have mean values $\overline{m}$ and $\overline{o}$, and standard deviations S_m and S_o, respectively. Performance levels were categorized as: >0.65 excellent; 0.65–0.5 very good; 0.5–0.2 good; <0.2 poor (Maréchal, 2004).

In general, the model showed similar simulations of salinity and current as the previous small domain model. The model showed reasonable skill scores for both salinity and tidal current (Table 2). For the salinity calibration, the SS at all stations was 0.71 at the surface and 0.76 at the bottom, which are within excellent score levels. SS for tidal current at all stations showed very good skill with scores of 0.63 and 0.68 at the bottom and surface, respectively. The CC values for both salinity and tidal current were high as expected. The CC and SS values indicate that the model had a good skill and the results were unbiased and acceptable.

4. Results

4.1. Morphological evolution

The sediment volume change was computed based on the spatially interpolated DEM. The result showed a vertical sediment accumulation in the study area (see rectangular area marked in Fig. 1) between 1986 and 2010. During the 1986–1997 period, the deposition area accounted for 64% of the entire area and the net accretion volume was 578×10^6 m^3. The net sediment accumulation rate during this period was 16.7 mm/year. Sediment accumulation was observed in the regions located seaward of North Channel, North Passage and Hengsha East Shoal (water depth >5 m). The net accretion thickness ranged from about 0.5 to 1.5 m. The region located seaward of Hengsha East Shoal experienced the most intensive deposition, with an accretion thickness exceeding 2 m over 1986–1997 (Fig. 3a).

The deposition area decreased to 57% of the study area and the net accretion volume decreased to 374×10^6 m^3 for the period 1997–2010. Meanwhile, the sediment accumulation rate decreased to 9.1 mm/year, which was about half of the accumulation rate during 1986–1997. Deposition mainly occurred on the shoals, especially in the Hengsha East Shoal, where accretion thickness reached up to 2 m. In contrast, two large erosion zones were aligned along the 10-m isobaths over the south-north direction in the submerged delta front. One region was located seaward of the North Channel (deeper than 10 m), and another region was located seaward of the North Passage and the South Passage (Fig. 3b). These erosion sites had been areas of deposition during the 1986–1997 period. This change from deposition to erosion has been attributed to sediment reduction after TGD when the riverine sediment supply to the delta failed to replenish the sediment removed from the delta (Yang et al., 2003). However, human intervention in the estuary may have also contributed to these changes, and we will present evidence for this below.

The shift of isobaths illustrates changes in the shoals and subaqueous delta in more detail. The shoals in the CJE experienced major deposition from 1986 to 2010 (Fig. 4). Here we used the 5-m isobaths to represent the area of the four main shoals in the CJE, which exhibited a continuous seaward expansion. Despite a dramatic decrease of riverine sediment during 1997–2010, the progradation rates in Hengsha East Shoal and Nanhui Shoal were higher than during1986–1997. The highest progradation rate was found to exist on the southern part of Hengsha East Shoal, which was behind the northern training wall of the DWP. The 10-m isobaths extended seaward for most of the subaqueous delta front from 1986 to 1997. The DWP significantly modified the 10-m isobaths between 1997 and 2010, reflected by the recession in the regions seaward of the Hengsha East Shoal and the South Passage. The 15-m isobaths were uniform compared with the 10-m isobaths, with slight seaward advancing between 1986 and 1997 and retreating landwards between 1997 and 2010.

Table 2
Correlation coefficient (CC) and skill score (SS) for the model.

	Salinity		Current	
	Surface	Bottom	Surface	Bottom
CC	0.9	0.93	0.89	0.86
SS	0.71	0.76	0.68	0.63

4.2. Tidal energy dissipation

The distributions of tidal energy dissipation computed by the model in the dry and wet seasons based on 1986 bathymetry are shown in Fig. 5a and e, respectively. As the tidal wave propagates into the CJE, the effect of bottom friction increases as water depth decreases. A notable increase of tidal energy dissipation occurs around the 10-m isobaths, which causes sediment resuspension and mixing along the isobaths. An analysis of historical bathymetric data reveals that the seabed around the 10-m isobaths has experienced marked shifting between deposition and erosion (Fig. 4), suggesting that the tide is one of the dominant forcings affecting the fluctuation of the delta front. The dominant tide in the CJE is the semidiurnal tide (M_2), which propagates in the SE-NW direction (305°) from the ocean. Therefore, a relatively high tidal energy dissipation occurs in the southern part of the CJE. The southern region is characterized as an active zone where suspended sediment and seabed sediment are exchanged frequently (Liu et al., 2010a, b). On the contrary, tidal energy dissipation is relatively weak in the northern portion of the CJE and high dissipation is restricted only along the 10-m isobaths. Large freshwater discharge acted as an additional energy source. Fluctuations of the river flow are seasonal and the interactions between freshwater and tides can alter tidal dissipation. During the dry season, when river discharge is relatively low, the tidal energy dissipation is more pronounced in the outer estuary and the high tidal dissipation zone extended further seaward (Fig. 5a). In the wet season, the increased river discharge suppresses the tidal current, which results in lower energy dissipation (Fig. 5e). Computed tidal energy dissipation in dry and wet seasons based on 1997 bathymetry is shown in Fig. 5b and f. Although the CJE experienced bathymetric changes due to sediment deposition during 1986–1997 (Fig. 3a), the spatial pattern of tidal energy dissipation is similar to the results of 1986.

Another calculation is completed by adding training walls and groins to the bathymetry of 1997. The results are shown in Fig. 5c and g for dry and wet seasons, respectively. After construction of the DWP, the training walls obstruct the tidal propagation, resulting in a sharp decrease in tidal energy dissipation in the lower reach of North Channel (north of the training wall), especially over the Hengsha East Shoal. In the southern region of the training walls between the North Passage and the South Passage, more energy dissipation is observed due to the enhanced flow caused by the training walls. The increase in dissipation suggests stronger interaction between currents and the seabed sediment and

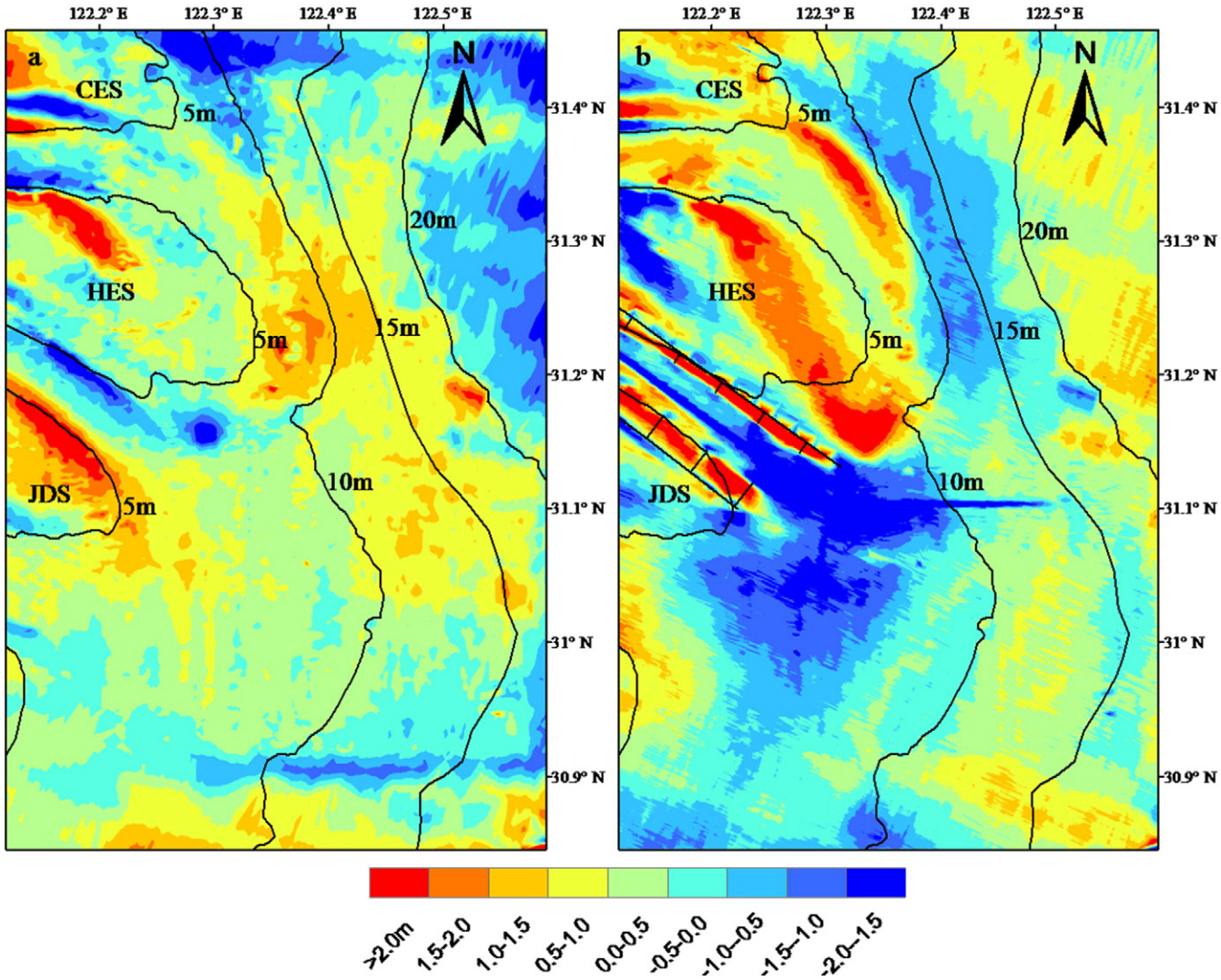

Fig. 3. Spatial distribution of erosion and deposition in the study area (a: 1986–1997, b: 1997–2010). Contours are the isobaths of 1997.

correspondingly more erosion is expected in these high-energy dissipation regions. The spatial distribution of tidal energy dissipation nicely corresponds to the erosion distribution between 1997 and 2010 (Fig. 3b).

The water depth increased in the subaqueous delta due to the erosion between 1997 and 2010. The increase of water depth reduces the bottom friction in the delta front, and results in less tidal energy dissipation (Fig. 5d, h). The change is more pronounced in the southern part below the confluence of the North Passage and the South Passage. As less energy is provided by the tidal current, a reduction of erosion is expected.

4.3. Erosion rate

Prior to the completion of the DWP, the results of erosion rate in 1986 (Fig. 6a, e) and 1997 (Fig. 6b, f) show a minor difference. In general, the erosion rate is relatively high in the southern part of the estuary, with the highest value approximately 1.0×10^{-4} kg·m^{-2}·s^{-1} in the channels. Similar to the tidal energy dissipation, the erosion rate decreased gradually seaward, suggesting less erosion occurred when water depth exceeded 20 m.

Seasonal variations of erosion rate were investigated by comparing the results between the dry (Fig. 6a, b) and wet (Fig. 6e, f) seasons. In the channels of the estuary, where the river discharge dominates the hydrodynamics, the erosion rate is higher during the wet season. While in the outer estuary, the large, buoyant river inputs suppress the tidal energy, resulting in less erosion at the seabed, especially in the region between the 10-m and 20-m isobaths. The seasonal variation of erosion rate suggests more sediment is eroded in the dry season. Historically, most sediment that deposited in the wet season in the subaqueous delta will be eroded in the dry season (Chen et al., 1988). Although the seasonal evolution pattern is mainly induced by winter storms (Wan et al., 2006), the interaction between river discharge and tide can also contribute to the erosion that occurred in winter.

The human impact was detected by running the model with training walls using the same bathymetry of 1997. The results of erosion rate in the dry season and the wet season are shown in Fig. 6c and g, respectively. The North Passage becomes narrow as a result of the training walls and groins and the flow concentrated in the deep channel. Compared with the model results without training walls, the tidal current out of the North Passage was enhanced and a region of high erosion rate was observed in the southern part of the training walls. For the region north of the training walls, the erosion rate slightly increased in the area between the 10-m and 20-m isobaths. The regions with increased erosion rate coincide with the areas of the CJE that were eroded following completion of the DWP, in both the southern and northern regions. North of the training wall where depths are <10 m, the erosion rate decreased sharply due to the obstruction on tidal propagation by the

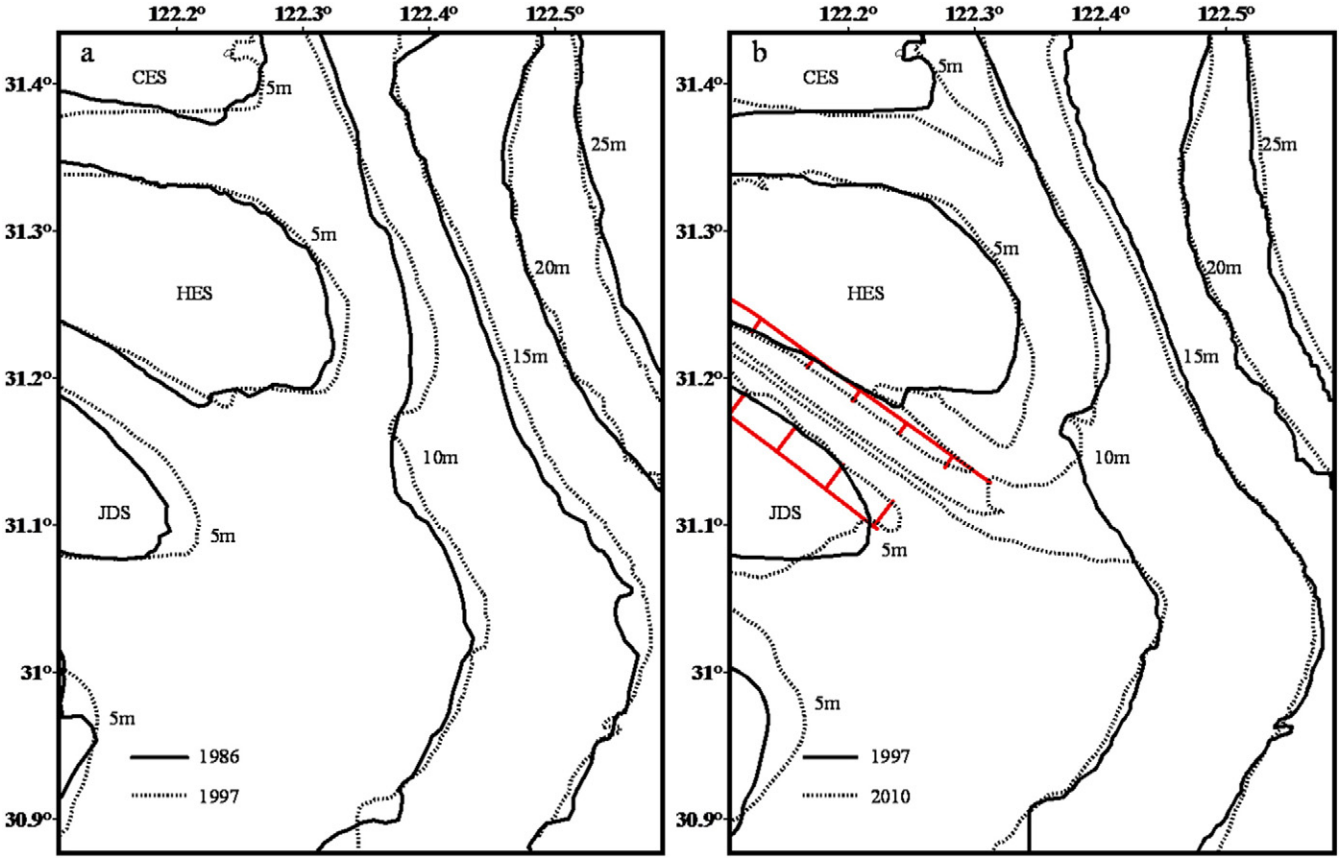

Fig. 4. Isobath movement in the study area (a: 1986–1997, b: 1997–2010).

training walls. Consequently, high deposition is expected to occur on the Hengsha East Shoal, and this agrees with the area of enhanced deposition recorded between 1997 and 2010. In general, the model indicates that a shifting between deposition and erosion can occur locally, even without any change of forcing and sediment supply.

The results presented in the previous section suggest that some regions of the CJE can undergo a period of erosion due to the increased erosion rate induced by the large estuarine infrastructure. After adjustment of the morphology, the erosion rate has been altered in the estuary. The erosion rate distributions using the 2010 bathymetry with training walls in dry and wet seasons are shown in Fig. 6d and h. After the intensive erosion occurred in the subaqueous delta, the erosion rate decreases in both the inner and the outer estuary. This result demonstrates that the erosion of the seabed may slow down gradually.

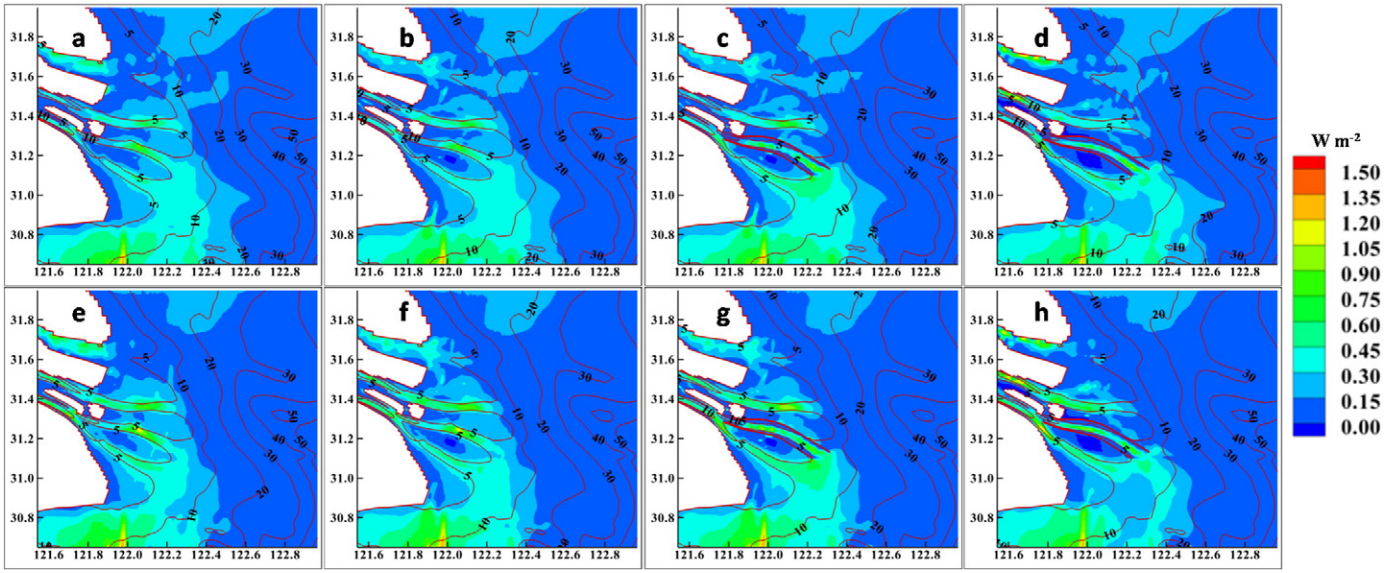

Fig. 5. Tidal energy dissipation in the Changjiang Estuary (top: dry season; bottom: wet season; a, e: 1986; b, f: 1997; c, g: 1997 with training walls; d, h: 2010). Contours are the isobaths in 1997.

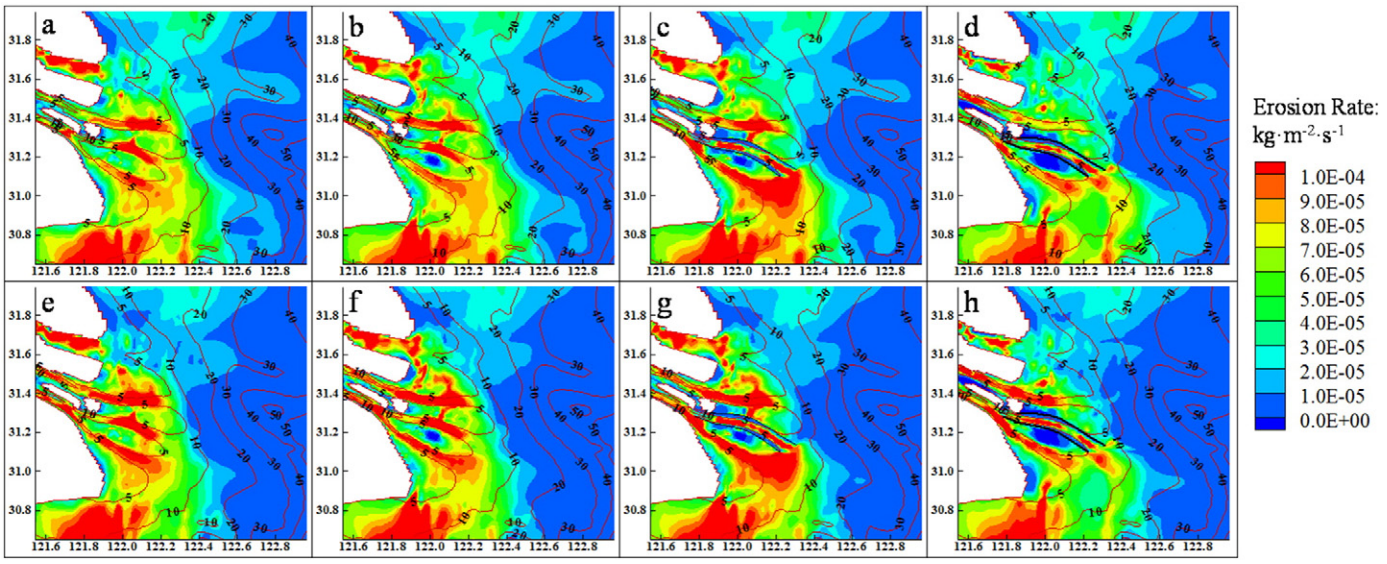

Fig. 6. Erosion rate distribution in the Changjiang Estuary (top: dry season; bottom: wet season; a, e: 1986; b, f: 1997; c, g: 1997 with training walls; d, h: 2010). Contours are the isobaths in 1997.

4.4. Residual currents

The residual current distribution is an indicator of net sediment transport. The residual current based on the 1997 bathymetry shows that there was frequent water and sediment exchange between the channels before the construction of the training walls (Fig. 7a, c). The surface residual current (Fig. 7a) in the North Channel is the strongest where it flows eastward and then southward in the subaqueous delta. The residual current at the mouth of the North Passage and the South Passage converge near the end of the channels between the 5-m and

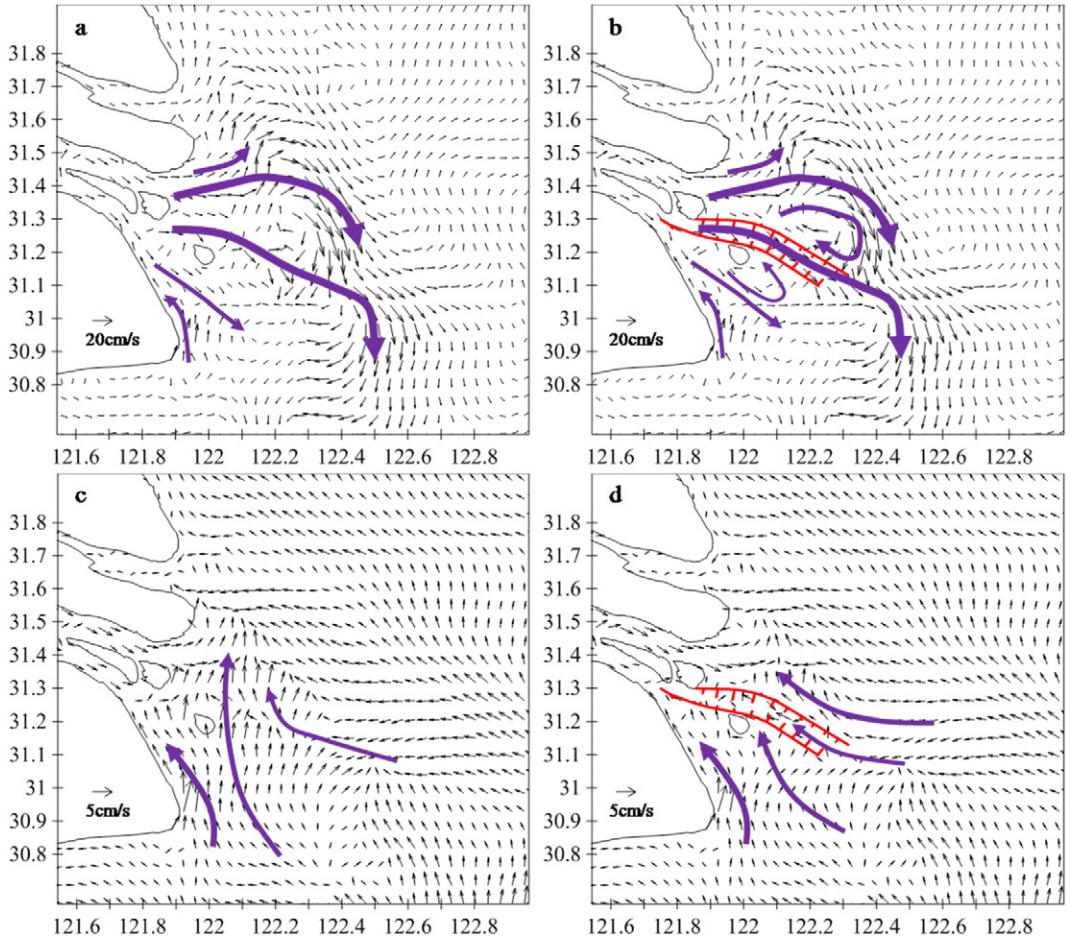

Fig. 7. M_2 tidal constituent-induced residual current in the dry season (top: surface residual current; bottom: bottom residual current; a, c: 1997; b, d: 1997 with training walls).

10-m isobaths in the subaqueous delta area. The structure of surface residual current suggests that the suspended sediment is transported out of the channels and has a tendency to be transported toward the south between the 5-m and 10-m isobaths. The bottom residual current (Fig. 7c) mainly flows westward from the marginal sea to the CJE. A portion of the bottom current is transported along the channel upstream. The remainder passes through the small channels across the shoals.

To investigate the impact of human intervention on residual currents, a model simulation with training walls using the bathymetry of 1997 was conducted. A large eddy is formed along the northern side of the training wall on Hengsha East Shoal (Fig. 7b). As a result of that, southward sediment movement was blocked, leading to fast accretion of the Hengsha East Shoal as indicated by a reduced erosion rate and manifested in the bathymetric changes (Fig. 3b). The water concentrated in the deeper part of the channel because of the narrowing effect of training walls and groins, enhancing residual current in the North Passage and its downstream reach. The southward residual current blocked a portion of the water from the South Passage, resulting in the formation of another eddy in the southern part of the training wall. The eddy has the tendency to trap more sediment inside the estuary. Furthermore, the enhanced landward bottom residual currents are induced by the narrowing channel and the increase of stratification in both the North Passage and the South Passage (Wang et al., 2010). More sediments have the tendency of being transported from the subaqueous delta to the mouth bar area. This suggests that the eroded sediment in the subaqueous delta can supply sediment to the inner estuary, acting as a considerable source sustaining the tidal flats progradation.

5. Discussion

5.1. Pattern of morphological evolution

Historically, the subaqueous delta is the main deposition zone for the riverine sediment (Milliman et al., 1985; Shen et al., 1986a, b). The sedimentation rate in the delta decreased in recent decades due to the reduction of sediment load. Between the 1950s and 1980s, when sediment flux into the CJE was approximately 470×10^6 t/year, analysis of sediment accumulation rates based on ^{210}Pb from several cores indicates that the annual accretion rate range from 30–50 mm/year (DeMaster et al., 1985). The annual sediment flux from the river into the estuary between 1986 and 1997 was 348×10^6 t/year and further declined to 217×10^6 t/year between 1997 and 2010. The CJE exhibited a continuous accretion between 1986 and 2010, whereas the accretion rate decreased from 16.7 mm/year to 9.1 mm/year during that time span. The overall decrease in accretion in the CJE for the last decade is mainly due to the long-term decrease in sediment flux. The deposition area was about 64% of the study area for the 1986–1997 period and transition zone of deposition to slight erosion started to occur seaward of the South Passage. The deposition area further declined to 57% of the study area for the 1997–2010 period and alteration of localized erosion and accretion were observed. Two large erosion areas formed around the northern part of the 10-m isobaths and southern part seaward of the North Passage and the South Passage, where tidal energy dissipation starts to increase due to the shallow water depth (Fig. 5). In the meantime, the tidal flats in the CJE experienced consistent accretion and progradation seaward. The erosion pattern from 1997 to 2010 differed from the historical pattern, which was mainly caused by the large constructions in the estuary.

5.2. Causes of morphological changes

The sediment flux from upstream has decreased since the 1980s (Fig. 2). The construction of reservoirs in the river basin has been proven to be the main factor leading to the sediment reduction, among which 32.2% of the sediment flux reduction is caused by the TGD, and the remaining 67.8% contributed by the other dams (Gao et al., 2015). Meanwhile, the suspended sediment grain size has decreased from 17 μm before 2003 to 10 μm due to erosion of fine bed sediment along the stretch between TGD and the estuary (Tang, 2007). There is no doubt that the reduction in sediment from the river basin has a long-term influence on the subaqueous delta (Gao, 2007). The decrease in the overall sedimentation rate in the delta has resulted from this long-term decrease of sediment load, whereas local changes of deposition/erosion are highly correlated with human activities in recent years, especially the DWP (Jiang et al., 2012). Increases in erosion rate induced by the DWP is detected in regions seaward of North Channel, North Passage, and South Passage (Fig. 8), whose patterns agree with the erosion patterns during the 1997–2010 period (Fig. 3b). In addition, the construction of the training walls also alters the dynamics of the shoals and the horizontal circulation pattern. Sediments tend to be trapped on the shoals. On the northern side of the training wall, a zone of marked deposition was formed, which corresponds to the area with a large decrease in erosion rate and the formation of an eddy of residual current. Consequently, the sediment supply to the deep water, offshore of the Hengsha Shoal (>10-m isobaths), is reduced. On the other hand, the erosion rate has increased in the deep water (>10-m isobaths). Combined with a decrease of sediment supply and an increase of erosion rate after the building the training wall (Fig. 8), erosion occurred over the offshore region of Hengsha East Shoal between the 10-m and the 20-m isobaths (Fig. 3b). Therefore, the influence of the TGD on the delta cannot be assessed

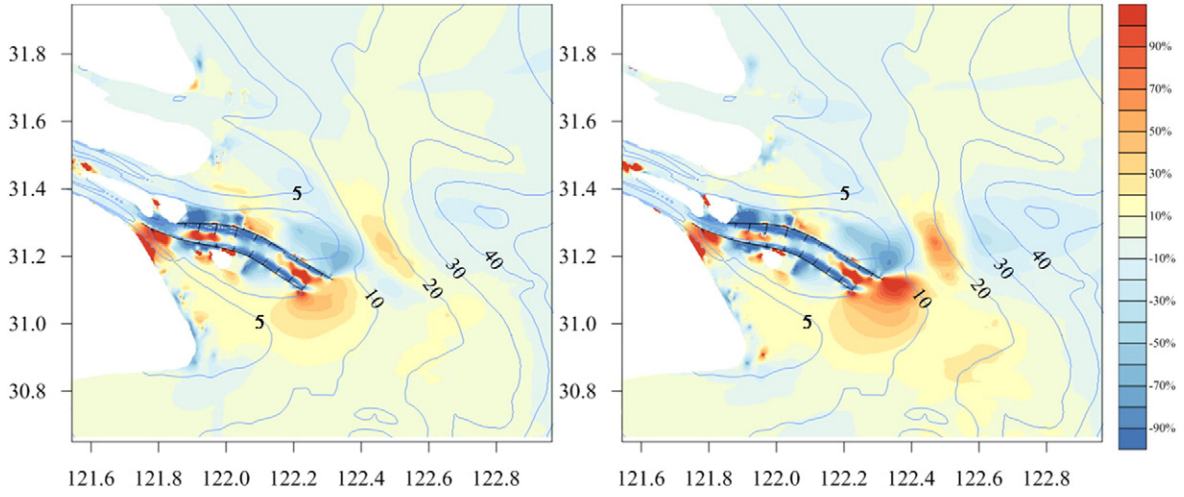

Fig. 8. Difference in erosion rate between model runs with and without training walls in 1997 (a: dry season; b: wet season). Contours are the isobaths in 1997.

without considering the impact of human influence in the estuary. As the sediment entering the estuary decreased, an overall decrease of the accretion rate has been observed. In the regional scale, the DWP has modified the hydrodynamics in the CJE and the model results indicate that human intervention is the controlling factor on the regional alternation of erosion and deposition.

5.3. Implications of changing sediment source

The sources of sediment entering the CJE are a key issue for developing a conceptual understanding of the morphological evolution of the system. The riverine sediment has long been considered as the main source to maintain the expansion of the CJE (Milliman et al., 1985). The riverine sediment is deposited in the nearshore zone seaward of North Channel, North Passage and South Passage, where the water depth is between 7 m and 25 m (Yun, 2004). However, due to the long-term reduction of sediment flux from the river basin since the 1980s, the subaqueous delta of the CJE has begun to recede in recent years (Yang et al., 2011). This retreat is particularly evident around the 10-m isobaths outside North Channel, North Passage and South Passage, which are the main outlets of water and sediment. By contrast, the inner estuary and the tidal flats are still advancing (Figs. 3b, 4b), even though the sediment flux has decreased from 348×10^6 t/year to 217×10^6 t/year. The progradation of the shoals may be partly due to sediment inputs from the delta front erosion. A similar phenomenon can also be observed in the suspended sediment concentration, which decreases in both the upstream and downstream of the estuary while there is no significant change in the turbidity maximum zone (Zhai et al., 2007). This phenomenon suggests that there exists a sediment exchange between the turbidity maximum zone and the subaqueous delta once the riverine sediment inputs decreased to a certain threshold value.

Sediment transport is accompanied with sorting, mixing, and exchange between suspended sediments and bed sediments. Frequent exchange between suspended sediments and bed sediments occurs in the muddy zone seaward of South Passage, where the exchange rate (between suspended sediment and bottom sediment) is >0.6 (Li et al., 2012; Liu et al., 2010a, b). The erosion rate distribution (Fig. 6) and morphology evolution (Figs. 3, 4) also suggest that sediment transport is active seaward of South Passage. However, under the combined effects of the decrease of river sediment input and the change of hydrodynamic conditions, large-scale erosion has occurred in the subaqueous delta. Fine-grained sediments are eroded and suspended to the water column. Consequently, the clay content in suspended sediment has increased from 27.4% to 33.0% (Liu et al., 2012). As the riverine sediment flux decreased, the replenishment of sediment from the estuarine system itself became an important source. The eroded sediments in the subaqueous delta is evidence for the sediment source transition from the river to the delta front. Meanwhile, the eroded sediments were transported into the inner estuary and a portion of them are deposited in the regions with weak dynamics condition, such as the tidal flats. The remainder could be trapped in the turbidity maximum zone by the increased gravitational circulation, sustaining a high suspended sediment concentration. Finally, the tidal flats continue progradation seaward and a decreasing trend in suspended sediment grain size has been observed (Luo et al., 2012). The previously deposited sediment operates like a 'sediment reservoir' and a regional shifting of sediment source-sink has occurred due to the changing hydrodynamics.

The current study focuses on the interaction between tide and change of bathymetry on the hydrodynamics in the CJE. The results show that tide plays a critical role in the morphodynamics in the estuary. Besides the tide, the wind-induced waves and swells also play important roles in sediment transport in shallow regions in the CJE (Fan et al., 2006). The wind-induced waves and their interaction with current should be studied in the future to fully understand the impact of dynamics on the morphology of the estuary.

6. Conclusions

In this study, we investigated the causes of the morphological evolution of the subaqueous delta in the CJE since 1986. Analysis of bathymetric data showed that extensive morphological changes have occurred in the CJE, with strong spatial variations in erosion and deposition. The overall accretion rate in the study area decreased from 16.7 mm/year (1986–1997) to 9.1 mm/year (1997–2010), which is ascribed to the reduced flux of riverine sediment over the past couple of decades. On the contrary, the spatial distribution of erosion and accretion between 1997 and 2010 is caused mainly by human intervention in the CJE. The model results indicate that the recent morphological change is highly correlated to the altered local hydrodynamic condition after completion of the DWP. The change in dynamics is quantified by using tidal dissipation and erosion rate. An increase in erosion rate around the 10-m isobaths is observed, which corresponds well with the location of the erosion zone between 1997 and 2010. Two eddies have formed on the northern and southern side of the training walls, resulting in accretion of the tidal flats. The eroded sediments in the outer estuary tend to be transported into the estuary, as indicated by the landward residual currents and become a new sediment source for the turbidity maximum zone to maintain a high suspended sediment concentration and deposition on the shoals, even though sediment from the river has fallen substantially. It is expected that the erosion along the subaqueous delta will continue and gradually slow down until the interaction between currents and seabed reaches a new equilibrium in the near future.

Acknowledgements

The study was funded by National Natural Science Foundation of China (Nos. 51320105005, 41276080 and 41506105), the non-profit water conservancy project of MWR (No. 201201070-03), China-Postdoc Fund (2015M580306) and funding for short-term overseas study supported by the graduate school of East China Normal University. We thank Mr. Mac Sisson for his internal reviewing and suggestions.

References

Allen, J., Somerfield, P., Gilbert, F., 2007. Quantifying uncertainty in high-resolution coupled hydrodynamic-ecosystem models. J. Mar. Syst. 64 (1), 3–14.
Argote, M.L., Amador, A., Lavín, M., Hunter, J.R., 1995. Tidal dissipation and stratification in the Gulf of California. J. Geophys. Res. 100 (C8), 16103–16118.
Blott, S.J., Pye, K., Van der Wal, D., Neal, A., 2006. Long-term morphological change and its causes in the Mersey Estuary, NW England. Geomorphology 81 (1), 185–206.
Boon, J.D., 2004. Secrets of the Tide: Tide and Tidal Current Analysis and Applications, Storm Surges and Sea Level Trends. Horwood Publishing (212 pp.).
Chen, J., 2007. Research and Practice of Estuary and Coast in China. Higher Education Press, Beijing, China (1015 pp. In Chinese).
Chen, X., Zong, Y., 1998. Coastal erosion along the Changjiang deltaic shoreline, China: history and prospective. Estuar. Coast. Shelf Sci. 46, 733–742.
Chen, J., Shen, H., Yun, C., 1988. Process of Dynamics and Geomorphology of the Changjiang Estuary. Shanghai Scientific and Technical Publishers, Shanghai, China (454 pp. In Chinese).
Chen, J., Li, D., Hu, F., Zhu, H., Liu, C., 1999. The processes of dynamic sedimentation in the Changjiang Estuary. J. Sea Res. 41, 129–140.
Codiga, D.L., Aurin, D.A., 2007. Residual circulation in eastern long island sound: observed transverse-vertical structure and exchange transport. Cont. Shelf Res. 27, 103–116.
Dai, Z., Liu, J.T., Wei, W., Chen, J., 2014. Detection of the Three Gorges Dam influence on the Changjiang (Yangtze River) submerged delta. Sci. Rep. 4 (6600), 1–7.
Davis, R.A., Hayes, M.O., 1984. What is a wave-dominated coast? Mar. Geol. 60, 313–329.
DeMaster, D.J., McKee, B.A., Nittrouer, C.A., Qian, J., Cheng, G., 1985. Rates of sediment accumulation and particle reworking based on radiochemical measurements from continental shelf deposits in the East China Sea. Cont. Shelf Res. 4, 143–158.
Fan, D., Guo, Y., Wang, P., Shi, J.Z., 2006. Cross-shore variations in morphodynamic processes of an open-coast mudflat in the Changjiang Delta, China: with an emphasis on storm impacts. Cont. Shelf Res. 26 (4), 517–538.
Galperin, B., Kantha, L.H., Hassid, S., Rosati, A., 1988. A quasi-equilibrium turbulent energy model for geophysical flows. J. Atmos. Sci. 45, 55–62.
Gao, S., 2007. Modeling the growth limit of the Changjiang Delta. Geomorphology 85, 225–236.
Gao, S., Wang, Y., Gao, J., 2011. Sediment retention at the Changjiang sub-aqueous delta over a 57 year period, in response to catchment changes. Estuar. Coast. Shelf Sci. 95, 29–38.

Gao, J., Jia, J., Kettner, A.J., Xing, Wang, Y., Li, J., Bai, F., Zou, X., Gao, S., 2015. Reservoir-induced changes to fluvial flux and their downstream impacts on sedimentary processes: The Changjiang (Yangtze) River, China. Quat. Int. (in press).
Ge, J., Chen, C., Qi, J., Ding, P., Beardsley, R.C., 2012. A dike–groyne algorithm in a terrain-following coordinate ocean model (FVCOM): development, validation and application. Ocean Model 47, 26–40.
Hamrick, J.M., 1996. User's manual for the environmental fluid dynamics computer work. Virginia Institute of Marine Science/School of Marine Science, the College of William and Mary. Special Report in Applied Marine Science and Ocean Engineering No. 331.
Hori, K., Saito, Y., Zhao, Q., Cheng, X., Wang, P., Sato, Y., Li, C., 2001. Sedimentary facies and Holocene progradation rates of the Changjiang (Yangtze) delta, China. Geomorphology 41, 233–248.
Hu, K., Ding, P., 2009. The effect of deep waterway constructions on hydrodynamics and salinities in Yangtze Estuary, China. J. Coast. Res. 2, 961–965.
Hu, K., Ding, P., Wang, Z., Yang, S., 2009. A 2D/3D hydrodynamic and sediment transport model for the Yangtze Estuary, China. J. Mar. Syst. 77, 114–136.
Huang, J., 2003. The Characteristics of Suspended Sediment Transport Under Currents and Waves in Changjiang Estuary (Master's Thesis) East China Normal Univer., Shanghai, China (In Chinese).
Huang, H., Zhu, J., Wu, H., 2007. 3-D numerical simulation of storm surge in the Changjiang Estuary and the Hangzhou Bay. J. East China Norm. Univ. (Natur. Sci.) 4, 9–19 (In Chinese with English Abstract).
Huo, M., Fan, D., Lu, Q., Liu, A., 2010. Decadal variations in the erosion/deposition pattern of Nanhui muddy bank and their mechanism in the Changjiang Delta. Acta Oceanol. Sin. 32 (5), 41–51 (In Chinese, with English Abstract).
Jayne, S.R., Laurent, L.C.S., 2001. Parameterizing tidal dissipation over rough topography. Geophys. Res. Lett. 28 (5), 811–814.
Jeong, S., Yeon, K., Hur, Y., Oh, K., 2010. Salinity intrusion characteristics analysis using EFDC model in the downstream of Geum River. J. Environ. Sci. 22 (6), 934–939.
Ji, Z.G., Morton, M., Hamrick, J., 2001. Wetting and drying simulation of estuarine processes. Estuar. Coast. Shelf Sci. 53 (5), 683–700.
Jiang, C., Li, J., de Swart, H.E., 2012. Effects of navigational works on morphological changes in the bar area of the Yangtze Estuary. Geomorphology 139–140, 205–219.
Kennish, M.J., 2001. Coastal salt marsh systems in the U.S.: a review of anthropogenic impacts. J. Coast. Res. 17 (3), 731–748.
Kong, L., Qi, D., Wan, Y., Wang, W., Gu, F., 2010. Numerical simulation of wave field in the Yangtze Estuary. Port Waterw. Eng. 2 (438), 46–49 (In Chinese with English Abstract).
Li, J., Zhang, C., 1998. Sediment resuspension and implication for turbidity maximum in the Changjiang Estuary. Mar. Geol. 148, 117–124.
Li, C., Yang, S., Fan, D., Zhao, J., 2004. The change in Changjiang suspended load and its impact on the delta after completion of Three Gorges Dam. Quat. Sci. 24 (5), 495–500 (In Chinese, with English Abstract).
Li, P., Yang, S., Milliman, J., Xu, K., Qin, W., Wu, C., Chen, Y., Shi, B., 2012. Spatial, temporal, and human-induced variations in suspended sediment concentration in the surface waters of the Yangtze Estuary and adjacent coastal areas. Estuar. Coasts 35 (5), 1316–1327.
Lin, J., Kuo, A.Y., 2003. A model study of turbidity maxima in the York River Estuary, Virginia. Estuaries 26 (5), 1269–1280.
Liu, J., Li, A., Xu, K., Velozzi, D., Yang, Z., Milliman, J., DeMaster, D., 2006. Sedimentary features of the Yangtze River-derived along-shelf clinoform deposit in the East China Sea. Cont. Shelf Res. 26 (17), 2141–2156.
Liu, Y., MacCready, P., Hickey, B.M., Dever, E.P., Kosro, P.M., Banas, N.S., 2009. Evaluation of a coastal ocean circulation model for the Columbia River plume in summer 2004. J. Geophys. Res. Oceans (1978–2012) 114 (C2).
Liu, H., He, Q., Wang, Z., Weltje, G.J., Zhang, J., 2010a. Dynamics and spatial variability of near-bottom sediment exchange in the Yangtze Estuary, China. Estuar. Coast. Shelf Sci. 86 (3), 322–330.
Liu, S., Yu, W., Kuang, C., Sun, B., 2010b. Preliminary prediction on recent topography evolution of Nanhui tidal flat in Yangtze Estuary due to Three Gorges project. J. Tongji Univ. (Natur. Sci.) 38 (5), 679–684 (In Chinese with English Abstract).
Liu, G., Zhu, J., Wang, Y., Wu, H., Wu, J., 2011. Tripod measured residual currents and sediment flux: impacts on the silting of the deepwater navigation channel in the Changjiang Estuary. Estuar. Coast. Shelf Sci. 93, 192–201.
Liu, H., He, Q., Wang, Y., Chen, J., 2012. Process of suspended sediment mixture in the Yangtze River Estuary. Acta Geograph. Sin. 67 (9), 1269–1281 (In Chinese with English Abstract).
Luo, X.X., Yang, S.L., Zhang, J., 2012. The impact of the Three Gorges Dam on the downstream distribution and texture of sediments along the middle and lower Yangtze River (Changjiang) and its estuary, and subsequent sediment dispersal in the East China Sea. Geomorphology 179, 126–140.
Ma, G., Shi, F., Liu, S., Qi, D., 2011. Hydrodynamic modeling of Changjiang Estuary: model skill assessment and large-scale structure impacts. Appl. Ocean Res. 33 (1), 69–78.
Ma, G., Shi, F., Liu, S., Qi, D., 2013. Migration of sediment deposition due to the construction of large-scale structures in Changjiang Estuary. Appl. Ocean Res. 43, 148–156.
Maréchal, D., 2004. A Soil-Based Approach to Rainfall-runoff Modelling in Ungauged Catchments for England and Wales (Ph.D. Thesis) Cranfield Univer., Cranfield, U. K.
Mellor, G.L., Yamada, T., 1982. Development of a turbulent closure model for geophysical fluid problems. Rev. Geophys. Space Phys. 20 (4), 851–875.
Milliman, J.D., Shen, H., Yang, Z., Meade, R.H., 1985. Transport and deposition of river sediment in the Changjiang and its adjacent continental shelf. Cont. Shelf Res. 4, 37–45.
Mulder, H.P., Udink, C., 1990. Modelling of cohesive sediment transport. A case study: the western Scheldt estuary. Coast. Eng. Proc. 1 (22).
Murphy, A.H., 1988. Skill scores based on the mean square error and their relationships to the correlation coefficient. Mon. Weather Rev. 116 (12), 2417–2424.
Nichols, M.M., Howard-Strobel, M.M., 1991. Evolution of an urban estuarine harbor: Norfolk, Virginia. J. Coast. Res. 7 (3), 745–757.
Oke, P.R., Allen, J., Miller, R., Egbert, G., Austin, J., Barth, J., Boyd, T., Kosro, P., Levine, M., 2002. A modeling study of the three-dimensional continental shelf circulation off Oregon. Part I: model-data comparisons. J. Phys. Oceanogr. 32 (5), 1360–1382.
Park, K., Jung, H.S., Kim, H.S., Ahn, S.M., 2005. Three-dimensional hydrodynamic-eutrophication model (HEM-3D): application to Kwang-Yang Bay, Korea. Mar. Environ. Res. 60 (2), 171–193.
Partheniades, E., 1962. A Study of Erosion and Deposition of Cohesive Soils in Salt Water (Ph.D. Thesis) University of California, Berkeley (182 pp.).
Shen, H., Li, J., Zhu, H., Zhou, F., 1986a. Transport of the suspended sediments in the Changjiang Estuary. J. Sediment. Res. 1, 1–13 (in Chinese with English abstract).
Shen, H., Zhu, H., Mao, Z., 1986b. Circulation of the Changjiang River Estuary and its effect on the transport of suspended sediment. Oceanol. Limnol. Sin. 17 (1), 26–35 (in Chinese with English abstract).
Shen, F., Zhou, Y., Li, J., He, Q., Verhoef, W., 2013. Remotely sensed variability of the suspended sediment concentration and its response to decreased river discharge in the Yangtze estuary and adjacent coast. Cont. Shelf Res. 69, 52–61.
Sherwood, C.R., Jay, D.A., Harvey, R.B., Hamilton, P., Simenstad, C.A., 1990. Historical changes in the Columbia River estuary. Prog. Oceanogr. 25 (1), 299–352.
Spearman, J., Dearnaley, M., Dennis, J., 1998. A simulation of estuary response to training wall construction using a regime approach. Coast. Eng. 33 (2), 71–89.
Stone, R., 2008. Three Gorges Dam: into the unknown. Science 321, 628–632.
Syvitski, J.P.M., Kettner, A.J., Overeem, I., Hutton, E.W.H., Hannon, M.T., Brakenridge, G.R., Day, J., Vörösmarty, C., Saito, Y., Giosan, L., Nicholls, R.J., 2009. Sinking deltas of human activities. Nat. Geosci. 2, 681–686.
Talke, S.A., de Swart, H.E., Schuttelaars, H., 2009. Feedback between residual circulations and sediment distribution in highly turbid estuaries: an analytical model. Cont. Shelf Res. 29 (1), 119–135.
Tang, J., 2007. Characteristics of Fine Cohesive Sediment's Flocculation in the Changjiang Estuary and its Adjacent Sea Areas (Master's Thesis) East China Normal University, Shanghai, China (In Chinese).
Tang, J., He, Q., Wang, Y., Liu, H., 2008. Study on in-situ flocs size in turbidity maximum of the Changjiang Estuary. J. Sediment. Res. 2, 27–33 (in Chinese with English Abstract).
Wan, X., Li, J., Shen, H., 2006. Distribution and diffusion of suspended sediment in the offshore area of Changjiang Estuary, China. Geogr. Res. 25 (2), 294–302 (In Chinese with English Abstract).
Wang, Y., Shen, J., He, Q., 2010. A numerical model study of the transport timescale and change of estuarine circulation due to waterway constructions in the Changjiang Estuary, China. J. Mar. Syst. 82 (3), 154–170.
Wang, Y., Shen, J., He, Q., Zhu, L., Zhang, D., 2015. Seasonal variations of transport time of freshwater exchanges between Changjiang Estuary and its adjacent regions. Estuar. Coast. Shelf Sci. 157, 109–119.
Webster, R., Oliver, M.A., 2007. Geostatistics for Environmental Scientists. John Wiley & Sons, Chichester, UK (271 pp.).
Wu, H., Zhu, J., Ho Choi, B., 2010. Links between saltwater intrusion and subtidal circulation in the Changjiang Estuary: a model-guided study. Cont. Shelf Res. 30 (17), 1891–1905.
Wu, J., Liu, J.T., Wang, X., 2012. Sediment trapping of turbidity maxima in the Changjiang Estuary. Mar. Geol. 303–306, 14–25.
Xiao, W., Ding, P., Hu, K., 2008. Numerical calculation of wave fields with tide and currents in Yangtze Estuary. Ocean Eng. 26 (4), 45–52 (In Chinese with English Abstract).
Xie, R., Wu, D.-A., Yan, Y.-X., Hai, Z., 2010. Fine silt particle pathline of dredging sediment in the Yangtze River deepwater navigation channel based on EFDC model. J. Hydrodyn. Ser. B 22 (6), 760–772.
Xu, J., He, Q., Wang, Y., 2009. Application of instrumented tetrapod in bottom boundary layer for water-sediment measurement. Ocean Eng. 27 (1), 55–61 (In Chinese with English Abstract).
Yang, S., Ding, P., Chen, S., 2001. Changes in progradation rate of the tidal flats at the mouth of the Changjiang (Yangtze) River, China. Geomorphology 38, 167–180.
Yang, S.L., Belkin, I.M., Belkina, A.I., Zhao, Q.Y., Zhu, J., Ding, P.X., 2003. Delta response to decline in sediment supply from the Yangtze River: evidence of the recent four decades and expectations for the next half-century. Estuar. Coast. Shelf Sci. 57 (4), 689–699.
Yang, S.L., Milliman, J.D., Li, P., Xu, K., 2011. 50,000 dams later: erosion of the Yangtze River and its delta. Glob. Planet. Chang. 75, 14–20.
Yun, C., 2004. Recent Development of the Changjiang Estuary. China Oceanpress, Beijing, China (290 pp. In Chinese).
Zhai, X.M., He, Q., Liu, H., 2007. Characteristics of current and sediment in the Changjiang Estuary during the dry seasons. Mar. Sci. Bull. 26 (4), 23–33 (In Chinese with English Abstract).